Plunger Kinematic Parameters Affecting Quality of High-Pressure Die-Cast Aluminum Alloys

ELENA FIORESE and FRANCO BONOLLO

The selection of the optimal process parameters in high-pressure die casting has been long recognized as a complex problem due to the involvement of a large number of interconnected variables. Among these variables, the effect of the plunger motion has been proved to play a prominent role, even if a thorough and exhaustive study is still missing in the literature. To overcome this gap, this work aims at identifying the most relevant plunger kinematic parameters and estimates their correlation with the casting quality, by means of a statistically significant sample manufactured with different plunger motion profiles. In particular, slow and fast shot velocities and switching position between two stages have been varied randomly in accordance with design of experiment methodology. The quality has been assessed through the static mechanical properties and porosity percentage. As a further proof, the percentage of oxides has been estimated on the fracture surfaces. These measurements have been correlated to novel parameters, representing the mechanical energy and the inertial force related to the plunger motion, that have been extracted from the time-history of the displacement curves. The application of statistical methods demonstrates that these novel parameters accurately explain and predict the overall quality of castings.

I. INTRODUCTION

HIGH-PRESSURE die casting (HPDC) is a cost-effective process widely used to manufacture components with high productivity and dimensional accuracy for automotive and other industries. The main disadvantages of this process are gas entrapment and oxide formation due to the highly turbulent flow of metal in the chamber and die cavity. The entrapped gas remains in the casting in the form of gas porosity which hinders the casting suitability for conventional heat treatment and deteriorates the casting quality sometimes to such a degree that it must be rejected.[1] Meanwhile, oxides worsen the tensile properties of the casting and cause premature failure.[2]

HPDC can be basically described through the sequence of three stages that can be easily recognized by analyzing the plunger motion profile and the pressure exerted by the hydraulic actuator. The first stage of the process, also called slow shot stage, requires usually constant and low speed for filling the shot sleeve and for avoiding turbulence in the melt and consequent generation of defects in the casting. The second stage, also called fast shot stage, is the filling of the die cavity, which should be performed at higher speed in order to avoid premature solidification at the gate and incomplete castings. Finally, the third stage, also called upset pressure stage, consists in applying an upset pressure on the solidifying melt in order to prevent the formation of shrinkage defects and the expansion of previously entrapped air.

The recent survey questionnaire addressed to the European foundries[3] and the extensive literature review[4] carried out by the authors have highlighted some critical issues that are yet unsolved. On the one hand, there is the actual need to improve the HPDC technology, since an average of 10 pct scrap is typically manufactured by this process due to the presence of porosity and oxides, which deteriorate the quality of castings.[3] On the other hand, there are no reliable methods in the existing literature to overcome this trouble and the available results are sometimes fragmented and conflicting.[4] Several works in the literature attempt to investigate this relevant issue, by examining the effect of different types of process characteristics on the final outcome.

Among the different critical process characteristics, several papers focus on the study of the so-called "process parameters" that are the modifiable settings of the injection machines. This approach aims at optimizing the quality of castings through the selection of the optimal machine settings, within those feasible, to ensure the best achievable performances given the melt chemical composition and the die geometry.

Among the HPDC process parameters investigated in the literature, particular attention has been paid to the so-called "kinematic parameters," *i.e.,* those related to the plunger motion. On the one hand, modifying the motion profile of the plunger is simple and costless, given the increasing use of highly automated and

ELENA FIORESE, Postdoctoral Fellow, and FRANCO BONOLLO, Full Professor, are with the Department of Management and Engineering, DTG University of Padova, Stradella S. Nicola 3, 36100, Vicenza, Italy. Contact e-mail: fiorese@gest.unipd.it.
Manuscript submitted October 27, 2015.
Article published online April 28, 2016.

servo-controlled injection machines which are capable of tracking desired motion profiles with high repeatability.[5] On the other hand, the plunger motion allows to explain several relevant phenomena, such as air entrapment, bubble collapse, as well as forces exerted on the melt, which are responsible for the casting quality, as it will be discussed in this work. An overview of the most important papers is proposed below, to review the state-of-the-art and to highlight the open issues.

Verran et al.[6] discussed the influence of two injection parameters, i.e., slow and fast shot speeds, on the internal quality of die-cast $Al_{12}Si_{1.3}Cu$ alloy. They have shown that the best results in terms of density were related to low speeds of slow (approximately equal to 0.14 m/s) and fast (approximately equal to 1.33 m/s) shots. They have demonstrated that the use of high speeds for the slow shot, as well as for the fast shot, increases turbulence in the liquid metal, thus causing air entrapment by the filling front and formation of porosity in castings. Dargusch et al.[7] examined the effects of different process parameters on the quality of castings in $Al_{13}Si_{0.3}Cu$ and Al_9Si_4Cu alloys. By investigating the influence of the casting velocity, porosity has been found to increase with increasing this parameter (in the range 1 to 3.8 m/s). Nevertheless, they have underlined that the variability of the data was large and more data were required to accurately demonstrate this trend.

Conversely, in the work of Gunasegaram et al.,[8] the analysis of tensile specimens of Al_8Si_3Cu alloy manufactured at three different melt flow velocities (varied in the range from 26 to 82 m/s) has revealed that the increase of the melt velocity results in finer microstructures and lower pore volume fraction and, consequently, better mechanical properties. Lumley et al.[9] investigated the influence of the melt velocity at the gate in die-cast Al_9Si_3Cu alloy. They have demonstrated that by increasing the melt velocity at the gate (varied in the range from 26 to 82 m/s), the probability of failure decreases due to the lower amount of porosity and oxides on the fracture surfaces of the tensile bars. Pałyga et al.[10] studied the effects of die casting process on the strength of castings in Al_9Si_3Cu alloy. It has been found that it is possible to specify a set of recommended settings of the second stage and the reduction of the predetermined setting leads to the formation of casting defects.

Guo et al.[11] focused on the effects of the process parameters on the metal–die interfacial heat transfer coefficient. They have demonstrated that the fast shot velocity positively affects the peak values of this coefficient. In accordance with this statement, Hamasaiid et al.[12] have found that higher second-stage velocities result in higher impact pressures, and these in turn result in higher values of both the heat transfer coefficient and the heat flux density.

Other papers focus on the sole first stage, by investigating the dynamic of the liquid metal flow as a function of the plunger speed and the possibility of air entrapment in the injection chamber.[13–15] Finally, some papers pay attention to non-physical schemes, such as neural networks and genetic algorithms or high-order response surfaces, to interpolate different combinations of some process parameters, such as first- and second-stage speeds.[16–20]

Although the existing literature provides interesting results, there are still some limitations and many papers often supply partial information for achieving an actual process optimization. In the following, a short description of these open issues is provided.

The first issue is the focus on instantaneous values of the process parameters. As already mentioned, many works in the literature usually focus on the influence of the first-stage constant speed and second-stage maximum speed. They usually consider just set or measured values of these parameters which are sometimes not exhaustive in representing the process.[6–10] Indeed, by assuming instantaneous values, it is neglected the integral nature of HPDC and the time-variability of speed during the process.

The second issue is the focus on just some stages of the process, particularly the first one.[13–15] Indeed, the amount of air entrapped during the first stage constitutes a considerable contribution to the overall entrapped air that causes porosity in castings. Nevertheless, the sole investigation of the first stage neglects the positive effects due to the forces exerted by the plunger on the melt in the second stage, which cause air bubble collapse and oxide fragmentation, with a consequent improvement of the static properties.

The last issue is the use of non-physical (such as neural networks and genetic algorithms) or high-order interpolation schemes.[16–20] Although these approaches are effective in the interpolation and useful for a specific case study, they could not provide hints to understand the parameters affecting quality in HPDC and to optimize them.

The aforementioned works of the existing literature give interesting contributions. Nevertheless, the definition of reliable criteria for tuning the HPDC parameters, in order to obtain sound and high-integrity castings, is still an open and challenging issue, which should be solved with a more comprehensive approach. In this context, the use of simplified behavioral models is very promising, which are abstract algebraic descriptions of HPDC representing the relation between some influential process parameters and quality of castings. To be effective, these simplified models should be, at the same time, capable of accounting for the physics and the integral nature of the process and its different stages.

Hence, the aim of this work is to identify the plunger kinematic parameters affecting quality of high-pressure die-cast aluminum alloys. In Section II, a novel approach based on numerical processing of signals is proposed for computing some novel kinematic parameters. This approach is then validated in Section III through an experimental activity and a thorough statistical analysis, which permit to identify some significant correlations between the novel kinematic parameters and the quality of the castings. In Section IV, conclusions from this work are drawn.

II. NOVEL PLUNGER KINEMATIC PARAMETERS

To solve the abovementioned issues, a new approach has been developed in this work, by overcoming the limitations of the use of either the slow shot (constant) speed or the fast shot (maximum and instantaneous) speed. The novel kinematic parameters proposed in this work take origin from some basic requirements.

First of all, the parameters should represent the main physical phenomena affecting the filling of the die/chamber and the solidification of the casting, and should have physical interpretation and statistical relevance. Clearly, HPDC is a complicated process, whose accurate explanation should involve models accounting for the fluid dynamic at the gate and inside the die cavity, by means of nonlinear differential equations. The proposed parameters are simplified representations of these complicated dynamic behaviors. As a consequence, since the filling of the die/chamber and the solidification of the casting is an "integral process" (in the mathematical sense) whose final outcome is expected to depend on the whole process or on some time intervals, the parameters should represent the time-history of the phenomenon, rather than just some instants. Hence, integral values of some signals computed over different time intervals are considered. Energy, as well as mean values over some time intervals, is expected to be suitable for the purpose.

To meet these requirements, it is expected that some parameters related to the plunger motion, which go beyond the simple measured position, could be effective. Therefore, the signals to be integrated will not belong to just the set of physical parameters that are directly measured by the sensors, *i.e.*, the position. In contrast, numerical derivatives of the displacement profiles will be employed to estimate speeds and accelerations, as well as other related physical quantities that represent fluid dynamic during HPDC process.

The use of signal processing is an effective tool to enlarge the set of data available and to provide a more exhaustive explanation of the phenomena. Clearly, the availability of effective and reliable numerical schemes to perform signal processing is of primary importance and allows to reduce the number of sensors to be employed, *e.g.*, by avoiding speed or acceleration direct measurements. In order to perform an accurate estimation of these parameters, by reducing the high-frequency noise usually introduced by numerical derivation,[21] an improved 7th-order Lanczos low-noise differentiator has been adopted, and is suggested, in accordance with the following scheme:

$$\dot{x}_k = \frac{3x_{k+3} + 2x_{k+2} + x_{k+1} - x_{k-1} - 2x_{k-2} - 3x_{k-3}}{28\Delta t},$$

[1]

where $\dot{x}_k$ and x_k denote the *k-th* sample of, respectively, the estimated speed and the measured position at time $k\Delta t$, with Δt the sample time. Obvious extension of Equation [1] is adopted to estimate acceleration $\ddot{x}_k$. Such a scheme has been applied in post-processing in a non-causal way (*i.e.*, it accounts for both previous and future samples), since it trades off very effectively between the need of smoothing the numerical noise and of ensuring an accurate estimation of the signal peaks with small computational effort.[21] Additionally, if it is applied in a causal way by just considering previous samples, it can be easily implemented online to perform real-time control and monitoring of the process with negligible time delay.

As an example, Figure 1 shows the measured plunger position and the computed speed and acceleration signals, taken from a sample casting among those analyzed in this work.

Starting from the speed and the acceleration estimations and from the careful identification of the most relevant physical phenomena (and their representation through algebraic models), two meaningful parameters have been finally defined and then experimentally validated through a rigorous statistical analysis which is reported in Section III. The two parameters proposed, which are novel in the metallurgy field, are the root mean square acceleration in the second stage and the integral of the cubic speed in the whole cycle. The mathematical and physical explanations of these parameters are provided and justified in Sections II–A and II–B.

A. *Root Mean Square Acceleration:* a_{RMS}

Since acceleration measurements are usually not provided by die casting machines, the effect of acceleration is rarely accounted for in the literature, except for vibrocasting processes[22] or for some works focusing on the effect of the transient acceleration on melt flow before the slow shot stage.[15] In contrast, attention is often paid to just the speed, regardless of its rate of variation over time. Hence, the information brought by some instantaneous values of speed is not always sufficient: the analysis of the Navier–Stokes's equations governing the motion of the melt clearly reveals that also acceleration plays an important role in describing the melt wave, whenever speed is not stationary.

On the other hand, acceleration sets the plunger inertial force and therefore represents the force transmitted to the melt by the plunger. Therefore, the analysis of this kinematic quantity supplies important information on the dynamic behavior of the fluid and on the balance of the forces. These reasons justify that acceleration should be considered as a meaningful parameter, as it will be corroborated by the statistical and metallurgical analyses.

In order to account for the whole second stage, the root mean square acceleration in the second stage is assumed as a representative parameter to describe and forecast the casting quality:

$$a_{RMS} = \sqrt{\frac{\int_{t_{s2}}^{t_{e2}} \ddot{x}(t)^2 dt}{t_{e2} - t_{s2}}}.$$

[2]

In Eq. [2], t is the time, $x(t)$ denotes the plunger displacement (and hence $\ddot{x}(t)$ the acceleration), and $t_{e2} - t_{s2}$ is the duration of the second stage (also
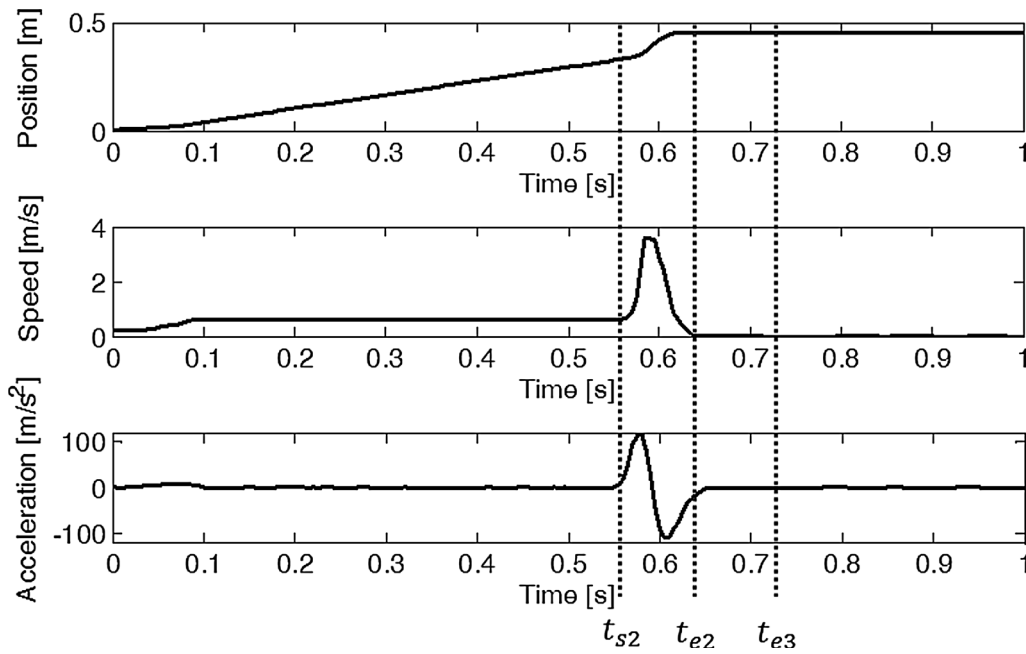
Fig. 1—Example of measured position and estimated speed and acceleration of the plunger during the process.

represented in Figure 1), which begins at $t = t_{s2} = t_{SW}$ (*i.e.,* the switching time), when the plunger reaches the switching position between the first and second stages, and ends when it reaches almost the final position at $t = t_{e2}$ (*i.e.,* the instant in which the second stage ends and the third stage starts). Equation [2] highlights also the integral nature of the parameter.

Physically, a_{RMS} represents the average value of the inertial forces (with unitary mass) of the plunger over the interval of integration. In practice, by expressing the Newtonian equilibrium of the plunger, it is also a measure of the force transmitted to the melt by the plunger during the second stage, which has been often recognized in the literature as the stage most affecting the final outcome.[23] By interpreting the RMS acceleration from a fluid dynamic point of view, it could be asserted that higher plunger accelerations imply higher forces that positively affect the filling of the die cavity and in turn improve the quality of castings (see Section III–B–3).

The use of the piston acceleration, rather than the acceleration of the fluid within the die cavity, is justified by theoretical and practical reasons. Indeed, the piston acceleration is related to the acceleration within the cavity. However, compared with the fluid acceleration, it can be easily measured (or estimated numerically) and also adopted for the a priori optimization of the process.

B. Parameter Representative of the Energy Associated to the Flow Forces: E_f

The second influential factor assumed to explain and predict the casting quality is a parameter representative of the energy associated to the flow forces, sometimes also denoted drag forces,[24] exchanged between the melt and the wall of the die/chamber, or exerted on solid

particles, such as oxides or inclusions, which are known to be preferential nucleation sites for porosity.[25] Since flow forces are proportional to the square velocity,[24,26] the power of these forces is proportional to the cubic velocity. Hence, the overall energy exerted is proportional to the integral of the cubic velocity over the whole cycle.

To account for the whole motion time of the plunger, integration of the cubic velocity has been performed over both the first and the second stages, *i.e.,* from time 0 to time t_{e2}, by leading to the following formulation:

$$E_f = \int_0^{t_{e3}} \dot{x}(t)^3 dt \cong \int_0^{t_{e2}} \dot{x}(t)^3 dt, \qquad [3]$$

where t is the time, $\dot{x}(t)$ denotes the plunger speed, and t_{e3} and t_{e2} are the instants in which the plunger reaches the end of the third and second stages, respectively (also shown in Figure 1). The two proposed formulations are in practice equivalent, because the speed in the third stage approaches zero.

The computation of the integrals has been performed numerically with the trapezoidal rule, in accordance with the following recursive scheme:

$$E_f(k) = E_f(k-1) + \Delta t \frac{\dot{x}(k)^3 + \dot{x}(k-1)^3}{2} \left(k = 1, \ldots, \frac{t_{e3}}{\Delta t} \right), \qquad [4]$$

where $E_f(k)$ is the integral value at time $k\Delta t$, while $\dot{x}(k)^3$ is the signal to be integrated. Clearly, the overall value is the last one computed, *i.e.,* $E_f = E_f\left(\frac{t_{e3}}{\Delta t}\right)$. Such a scheme has been adopted to ensure negligible signal drift, due to the unavoidable low-frequency noise usually introduced by numerical integration schemes, which imposes paying attention to numerical integration of measured noisy signals.[27]

From a fluid dynamic point of view, flow forces affect the melt behavior during the filling of both the chamber and the die cavity, by destabilizing the preferential nucleation sites for defects, thus enhancing the internal quality of castings (see Section III–B–3). Since the parameter E_f is an increasing function of the speed in both the first and second stages, it also summarizes those filling problems that are due to low values of speed, as often reported in the literature.[15]

A second physical interpretation can be given to the parameter E_f, according to Bernoulli principle. Indeed, E_f can be seen as a meaningful measure of the energy associated to the pressure forces in the whole cycle, since pressure variation is related to the square velocity.

Besides having two different and significant physical interpretations, this parameter deserves also a mathematical interpretation, in accordance with some works proposed in the literature showing that the second-stage speed has more influence compared with the one of the first stage.[23] The presence of the cubic exponent in the integral, as assumed in the novel parameter here proposed, gives higher importance to the higher speed values. The proposed parameter is therefore significantly affected by the peak speed and by the second-stage speed, but also accounts for the first stage.

Both the parameters have a meaningful fluid dynamic interpretation and represent two different phenomena that affect the final outcome of HPDC process. While a_{RMS} represents the average value of the force resultant in just the second stage, which is usually recognized in the literature as the most influential one, E_f represents the overall energy exerted by the flow forces inside the chamber/cavity in the whole process.

III. VALIDATION OF THE NOVEL PLUNGER KINEMATIC PARAMETERS

A. *Experimental Procedure*

For research purposes, a die for manufacturing horseshoe-shaped castings of aluminum alloy has been designed and developed in the frame of European Music project (MUlti-layers control & cognitive System to drive metal and plastic production line for Injected Components, N. 314145). The geometry of the casting has been designed in order to exacerbate the generation of defects, and therefore to study the effect of the process parameters on defects and overall casting quality (see Figure 2).

The manufacture process of the castings was realized at an industrial plant in a die casting cell, comprising a 7355 kN cold chamber die casting machine (shot chamber length 0.482 m and diameter 0.080 m), as well as a furnace and an automatic lubrication system for cooling down the die material and aiding the release of castings. The furnace was set to 978 K (705 °C), while the pouring temperature was approximately 45 deg lower. The temperature of the die was kept constant by a thermoregulation system. The temperature of the oil cooling channels was set to 518 K (245 °C) for the

Fig. 2—Horseshoe-shaped casting designed to exacerbate the generation of defects as a function of the process parameters.

moving half of the die, and to 508 K (235 °C) for the fixed half.

An $Al_9Si_3Cu(Fe)$ alloy was cast, corresponding to the EN AB-46000 aluminum alloy (European designation, equivalent to the US designation A380). A number of 15 to 20 castings were scrapped after start-up to obtain a quasi-steady-state temperature in the shot sleeve and the die.

Design of the experiment[28] has been planned, and then applied, by changing the slow and maximum fast shot speeds, the switching position between first and second stages, and the maximum upset pressure. These independent process parameters have been selected because they are simple to manipulate and to control, in accordance with those usually adopted by practitioners in planning the process. Each of the mentioned independent variables of the experiment, called control factor, has been varied within a feasible range, as large as possible. The values assumed by the control factors are given in Table I, by means of their lower and upper levels of observation, together with the discretization values. Only the first three parameters affect the motion profile of the plunger, and will be therefore accounted for in this investigation. In contrast, the upset pressure (which was varied from 50 to 100 MPa) will be only considered as a disturbance factor in this study.

The machine was instrumented with a position sensor recording the plunger displacement with sample time $\Delta t = 0.5e^{-3}$ seconds, and each casting is documented with its shot profile representing the plunger actual displacement curve. The motion of the servo-controlled plunger recalls the typical displacement curve, with an

initial transient before reaching the constant speed of the first stage, and then a second stage which follows a polynomial displacement profile. In contrast, no measurement of the time-history of the pressure was performed. Therefore, the upset pressure cannot be effectively investigated through an approach consistent with those proposed for studying the motion profile, since, in practice, just the set point value was available, rather than the complete time-history of the actual value. For this reason, upset pressure will be object of future investigations of the authors. However, it is well known in the literature, and also recognized by practitioners, that the application of high upset pressure has positive effects on the internal quality of castings. Indeed, high upset pressure prevents the formation of shrinkage porosity and the expansion of previously entrapped air during the casting solidification.[29]

A total amount of 32 different combinations of the control factors was tried, and each combination was manufactured with a number of repetitions ranging from 3 to 7. This set leads to a statistically significant sample (around 90 castings).

As for the dependent response variables, *i.e.,* the measured variables representing the casting quality (which should be correlated to the process parameters), both the peak load (representative of static mechanical properties) and the porosity percentage of the castings have been identified.

Bending test specimens were trimmed from the flat appendixes of the casting (Figure 3). Four specimens for each casting were drawn (with 0.04 m width, 0.002 m thickness, and 0.06 m length). The three-point bending test has been carried out with displacement control with a 4 mm/min rate and a rating force of 10 kN.

Moreover, the stepped wedge of the casting has been chosen for porosity measurements, as it was the most critical zone and emphasized the difference in quality level between castings obtained by different process parameters. The stepped wedge is a zone of the casting with the following dimensions: 0.059 m width, thickness ranging from 0.001 to 0.003 m, and 0.2 m length (Figure 4). The stepped wedges have been analyzed by a macro-focus X-ray equipment, whose settings were 60 kV and 1.5 mA, and the percentage of porosity has been then estimated by means of an image analysis software.

As a further proof, fracture surfaces of some selected castings have been also analyzed by scanning electron microscope and their percentage of oxides has been estimated by means of an image analysis software. Finally, the zone near the fracture surface has been analyzed by optical microscope in order to investigate which kinds of defects were present.

The rigorous application of statistical concepts, methods, and models, as well as the execution of thorough microscopic analyses, has been described in the following section to demonstrate that the novel kinematic parameters allow to explain and forecast both the static mechanical properties and the overall quality of castings. The coherence between exploratory and confirmatory analyses has also been assessed, to prove the reliability of the results obtained.

B. Correlation Between Plunger Kinematic Parameters and Quality

1. Correlation with the static peak load
In order to find some statistically significant correlations between the novel plunger kinematic parameters and the mechanical properties measured in the appendixes of the castings (see Figure 3), both exploratory and confirmatory analyses have been carried out, and coherence has been proven.

The exploratory analysis includes summary statistics (*i.e.,* minimum, maximum, median, 25th percentile, 75th percentile, mean, and standard deviation) and graphical displays of the data, such as boxplots, without making any assumption on distributions or models.[30]

The castings have been discriminated in two groups on the basis of their peak load, to analyze the summary statistics of the plunger kinematic parameters for the two groups. The first group collects the castings with peak load greater than 1.1 kN (see Table II), while the second one collects those with peak load lower or equal to this value (see Table III). The threshold of 1.1 kN corresponds to the median value of all the measured peak loads.

The boxplots of the two proposed parameters for the two groups of castings are represented in Figure 5. This

Table I. Control Factors with Their Lower and Upper Levels of Observation and Discretization Values

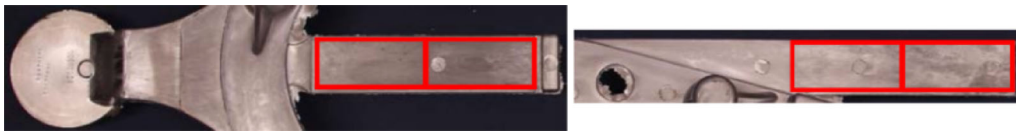| Control Factor	Low Level	High Level	Discretization
Slow shot speed (m/s)	0.2	0.8	0.1
Max fast shot speed (m/s)	1.5	4.0	0.5
Switching position (m)	0.30	0.35	0.01

Fig. 3—Position of specimens for bending test in the appendixes of the casting.

figure highlights that both a_{RMS} and E_{f} affect the peak load of the castings (referred to as F_{max}), since the interquartile ranges of the two groups are distinct. This is in particular true for a_{RMS}, where there is no overlap between the two groups. In contrast, the interquartile ranges are slightly overlapped in the case of E_{f}.

The results of the exploratory analysis have been also confirmed through the application of the formal statistical methods performed through the confirmatory analysis. Indeed, the t-tests executed on a_{RMS} and E_{f} confirm that there is true difference in means between the two groups of castings with 95 pct confidence interval and the p values are $8.4e^{-15}$ and $6.0e^{-10}$, respectively. p value measures the evidence that there is true difference in means between the two groups of castings: the smaller the p value is (particularly lower than 0.05), the stronger the evidence is.[30]

On the basis of the analysis of the boxplots and of the p values, and given the weak correlation between a_{RMS} and E_{f} in this specific set of data (although it is not true

Fig. 4—Position of specimen for radiographic testing in the stepped wedge of the casting.

in the general case, since these two parameters are mathematically different and represent two different physical phenomena), the fitting model has been developed by just assuming a_{RMS} as the sole independent variable. The correlation between such a parameter and the mechanical property is corroborated by Figure 6 which plots the exponential of the median peak load (denoted F_{max}) against this parameter, by means of the following fitting model:

$$\exp(F_{\mathrm{max}}) = \alpha_0 + \alpha_1 a_{\mathrm{RMS}}, \qquad [5]$$

where α_0 and α_1 are the scalar coefficients to be identified through least-square fitting.[31] The fitted coefficients for the alloy and the geometry investigated are as follows: $\alpha_0 = 2.40$ and $\alpha_1 = 0.014$. Clearly, the coefficients of the proposed behavioral model are related to the specific test case investigated. The result is however representative of the general case and reveals that quality improvement can be achieved by pushing the accelerations toward the highest feasible values. Whenever the proposed behavioral model should be employed with different geometries or alloys for process control or prediction, a preliminary model tuning would allow to estimate the correct model coefficients and hence to accomplish the task.

Figure 6 confirms that a_{RMS} affects the quality of castings and allows to explain the static mechanical properties: the higher a_{RMS} is, the higher the bending peak load is. This result can be reasonably justified, by

Table II. Summary Statistics of the Kinematic Parameters for Castings with Peak Load Greater than 1.1 kN

Parameter	Min	1st Qu.	Median	3rd Qu.	Max	Mean	St. dev.
a_{RMS} (m/s^2)	29.78	51.32	65.73	71.46	80.59	60.23	14.70
E_{f} (m^3/s^2)	0.36	0.75	1.21	1.39	2.09	1.14	0.45

Table III. Summary Statistics of the Kinematic Parameters for Castings with Peak Load Lower or Equal to 1.1 kN

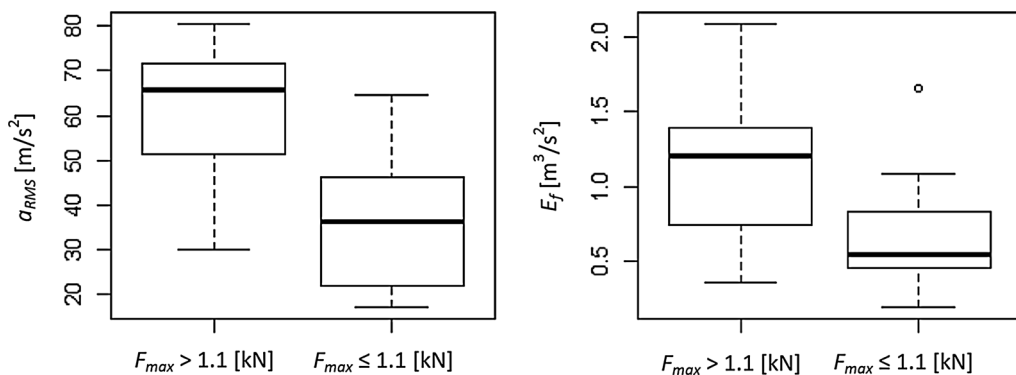| Parameter	Min	1st Qu.	Median	3rd Qu.	Max	Mean	St. Dev.
a_{RMS} (m/s^2)	17.11	21.84	36.09	46.36	64.57	34.80	12.50
E_{f} (m^3/s^2)	0.20	0.46	0.55	0.83	1.66	0.61	0.28

Fig. 5—Boxplots of a_{RMS} and E_{f} parameters for the two groups of castings, discriminated on the basis of bending peak load.

considering that higher accelerations mean higher forces transmitted by the plunger to the melt, which strive against oxides and fragment them (as it will be demonstrated in Section III–B–3).

The median value has been calculated between the peak loads of the four bending test specimens obtained from each casting. Indeed, the median value is more representative than the mean in the presence of outliers, due to random and uncontrolled exogenous factors. As for the fitting function, a logarithmic model has been assumed, to set a rate of growth that is "less than linear," so as to represent a decreasing rate of growth for high values of a_{RMS}, as it is reasonable. This assumption makes the model proposed more reasonable for being used in extrapolation. The resulting fitting model for a_{RMS} approximates the data distribution with a correlation coefficient equal to 0.66, which is a very satisfactory value.

The diagnostic plots (see Figure 7) highlight that this model fits the experimental data well: indeed, the residual plot does not show any pattern, and the quantile–quantile plot shows normality since its points do not deviate from a straight line.[32] The conclusions are reliable and convincing, as the results from exploratory and confirmatory analyses are in agreement.

It is also worth mentioning that assuming a power relation between the dependent and the independent variables, of the type $F_{max} = \alpha_0 a_{RMS}^{\alpha_1}$ (as often done in other fields of engineering), leads to a 0.64 correlation coefficient. Hence, both the models can be adopted effectively.

Although the values of correlation obtained do not approach the ideal target of 1, they should be assumed as very satisfactory, since they have been computed through a relevant number of samples (around 90 castings) and in the presence of the unavoidable uncertainty and disturbance of exogenous factors, affecting the HPDC process. Among the disturbance factors, it should be accounted for the role of the upset pressure, as discussed in Section III–A, which is not uniform between the castings. The effect of this parameter, which cannot be regarded as a kinematic parameter, will be object of further investigations through a different set of castings, where the time-history of the upset pressure will be available to provide a more rigorous discussion.

2. Correlation with the percentage of porosity

The same approach proposed in Section III–B–1 has been applied in order to find some statistically significant correlations between the novel plunger kinematic parameters and the percentage of porosity.

The castings have been discriminated in two groups on the basis of their percentage of porosity, to analyze the summary statistics of the two proposed parameters for the two groups. The first group collects the castings with percentage of porosity lower or equal to 2 pct, while the second one collects those with porosity greater than this value. Based on a common practice, a reasonable and conservative threshold of 2 pct porosity has been chosen to discriminate sound and poor castings.[33] However, the choice of the suitable threshold depends on the final application of castings.

The boxplots of the two proposed parameters for the two groups of castings are represented in Figure 8. This figure highlights that both the proposed parameters significantly affect the porosity of the castings (referred to as *Porosity*), since the interquartile ranges of the two groups are markedly distinct.

The results of the exploratory analysis have been also confirmed through the application of the formal statistical methods. The t-tests performed on a_{RMS} and E_f demonstrate that there is true difference in means between the sound and poor castings with 95 pct confidence interval and the p values are $2.8e^{-8}$ and $5.4e^{-4}$, respectively. Once again, a_{RMS} is the parameter most influencing the casting quality. However, with respect to the peak load, the boxplots are in this case completely separated for both the parameters, and hence multivariable models can be developed.

If a fitting model relating the natural logarithm of the porosity against a_{RMS} is assumed, an effective prediction is provided:

$$\log(\text{Porosity}) = \alpha_0 + \alpha_1 a_{RMS}. \quad [6]$$

The fitted coefficients for the alloy and the geometry investigated are as follows: $\alpha_0 = 4.42$ and $\alpha_1 = -0.08$. The fitting model approximates the data distribution with a correlation coefficient equal to 0.63, which is highly satisfactory. Indeed, porosity is often significantly affected by casual exogenous factors that cannot be monitored or predicted. Hence, castings having the same combination of the control factors in the design of experiment, and almost identical time-histories of the measured signal, sometimes had remarkably different values of porosity.

Figure 9 confirms that a_{RMS} positively affects also the porosity of castings: the higher a_{RMS} is, the lower the percentage of porosity is, since higher accelerations mean higher forces that make previously formed air bubbles collapse.

It is worth mentioning that porosity was measured in a different region of the casting with respect to the one used for measuring the static peak load. Hence, the proposed parameter provides a meaningful explanation of the overall casting quality.

If both a_{RMS} and E_f are taken into account in a multivariable model, a significant improvement is obtained, by leading to a 0.72 correlation coefficient and highlighting the influence also of the first stage, besides the second one, on the percentage of porosity. The final model proposed is as follows:

$$\log(\text{Porosity}) = \alpha_0 + \alpha_1 a_{RMS} + \alpha_2 E_f. \quad [7]$$

The diagnostic plots of this model (which have been omitted for brevity) are similar to those in Figure 7, and show that this model fits, once again, the experimental data well. The fitting model of Equation [7] is also represented in Figure 10. It can be seen that the plane of
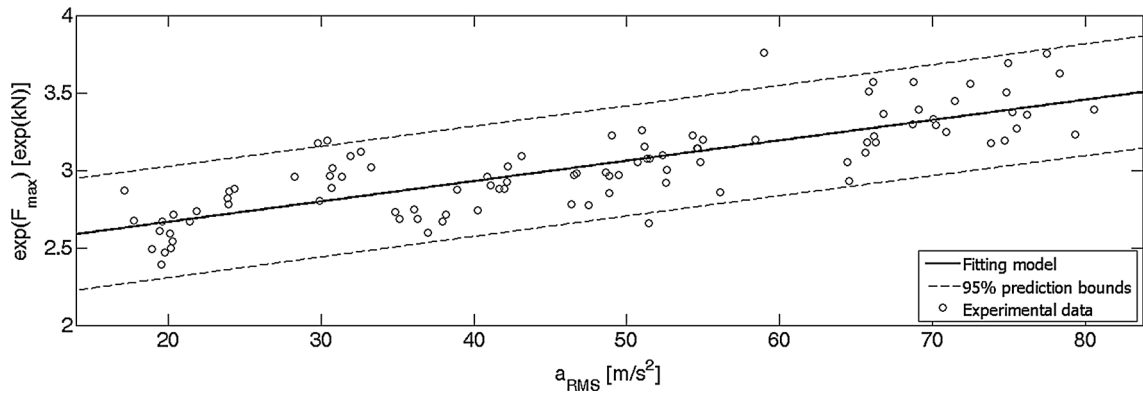
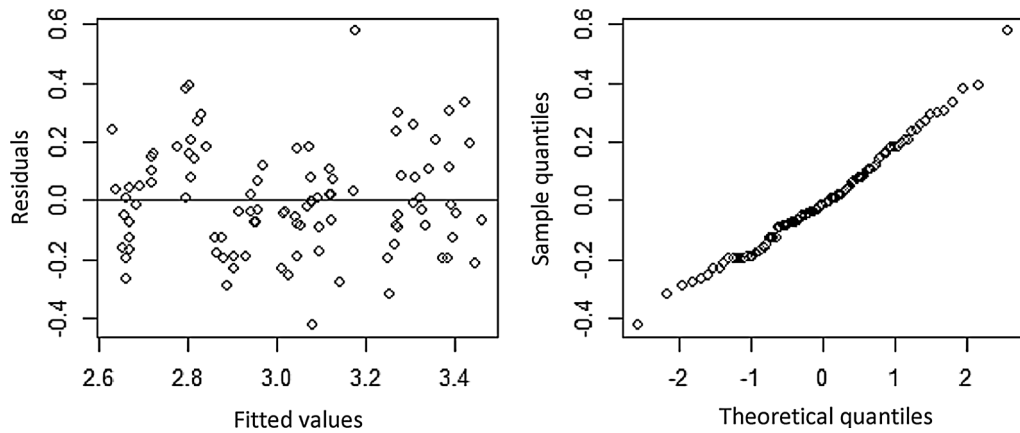Fig. 6—Bending peak load of the castings as a function of a_{RMS}.

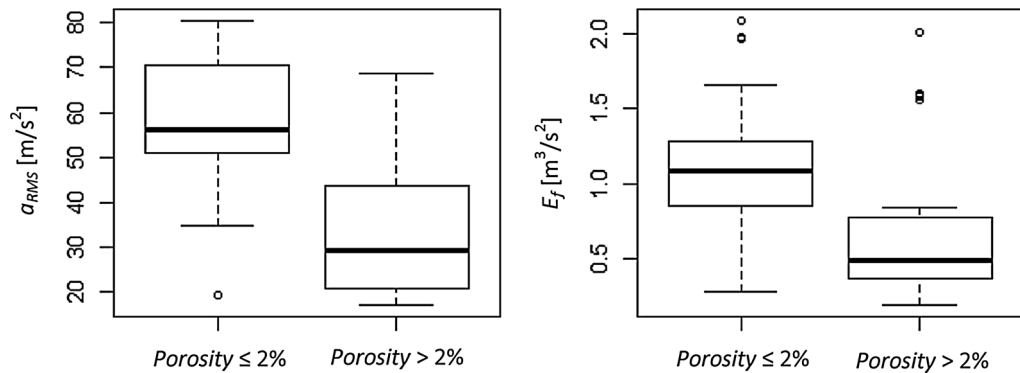Fig. 7—Residual plot and quantile–quantile plot of the model in Eq. [5].

Fig. 8—Boxplots of a_{RMS} and E_f parameters for the two groups of castings, discriminated on the basis of percentage of porosity.

the regression model fits effectively the experimental data.

3. Analysis of internal defects

As a further evidence of the correctness of the proposed approach in explaining the overall casting quality, fracture surfaces of some selected castings have been analyzed by scanning electron microscope (SEM) and their percentage of oxides has been estimated by means of an image analysis software. The aim of this analysis is to show the effect on the percentage of oxides

of an increase of a_{RMS} and E_f, by analyzing some castings with increasing values of these parameters, and therefore with increasing values of F_{max}. The analysis reveals that by increasing a_{RMS} and E_f, the percentage of oxides decreases, as shown in Table IV. The correlation is justified by the fact that higher accelerations imply higher forces that fragment the oxides, thus promoting their partial dissolution into the melt and avoiding premature failure of castings. As for the other parameter, being the flow forces exchanged between the melt and the wall of the die/chamber, or exerted on solid
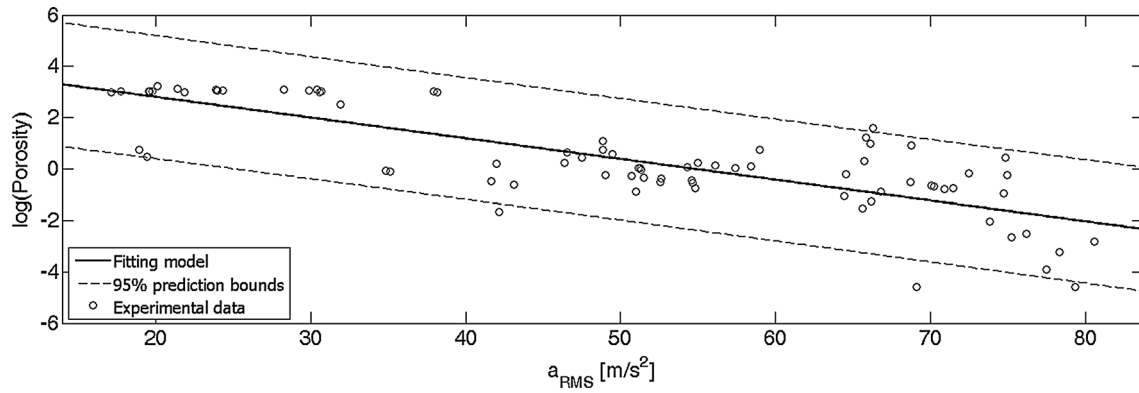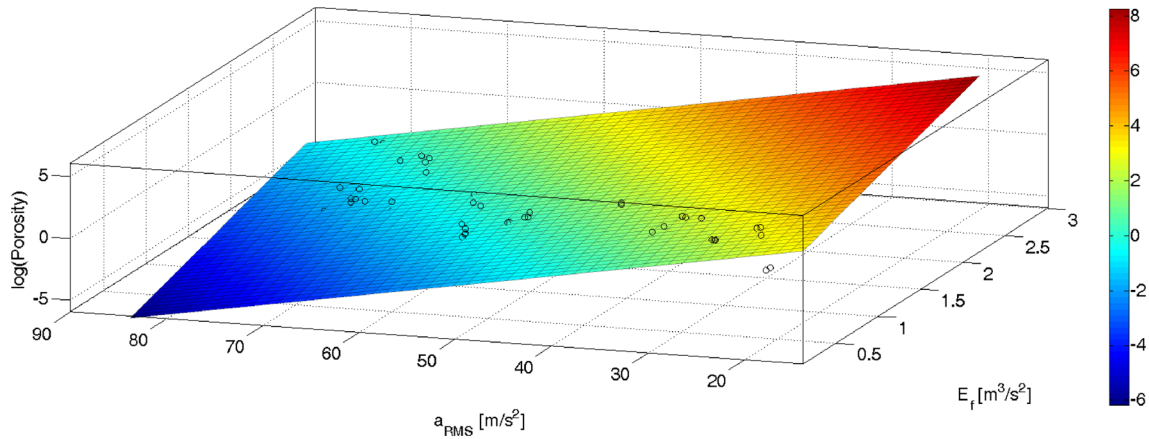
Fig. 9—Porosity of the castings as a function of a_{RMS}.

Fig. 10—Three-dimensional representation of the model in Eq. [7].

Table IV. Percentage of Oxides and Bending Peak Load as a Function of a_{RMS} and E_f

a_{RMS} (m/s²)	E_f (m³/s²)	F_{max} (kN)	Oxide (Percent)
20.25	0.45	0.93	9.12
36.33	0.56	0.99	4.75
46.55	0.93	1.09	1.69
50.73	1.04	1.12	0.88
71.46	1.41	1.24	0.18
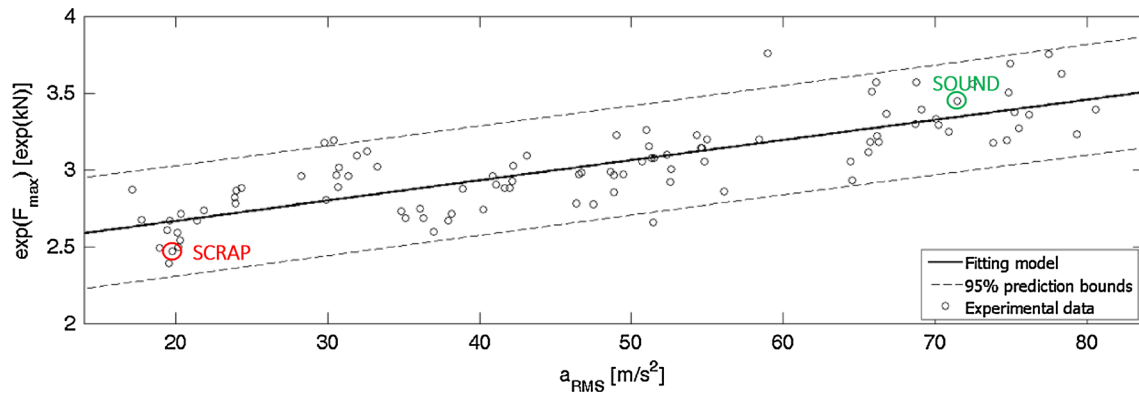
Fig. 11—Bending peak load of the castings as a function of a_{RMS}.
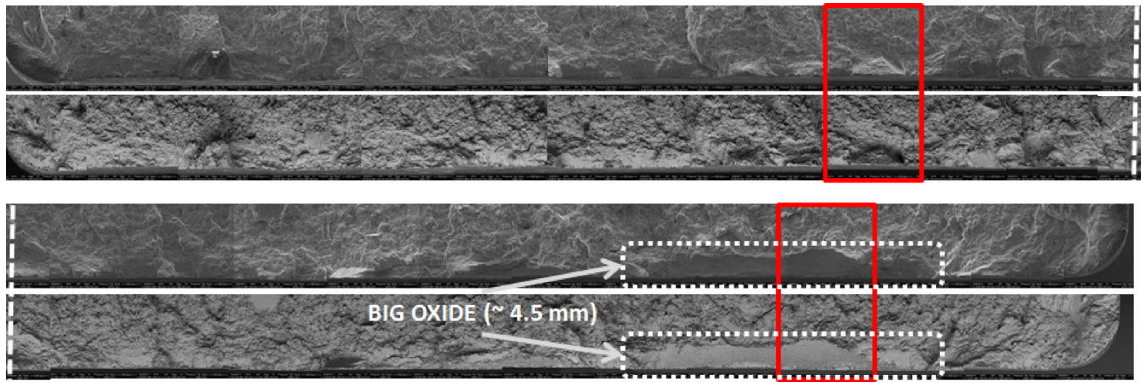
Fig. 12—SEM micrograph of the fracture surface of a scrap casting (a_{RMS} = 20.25 m/s^2).
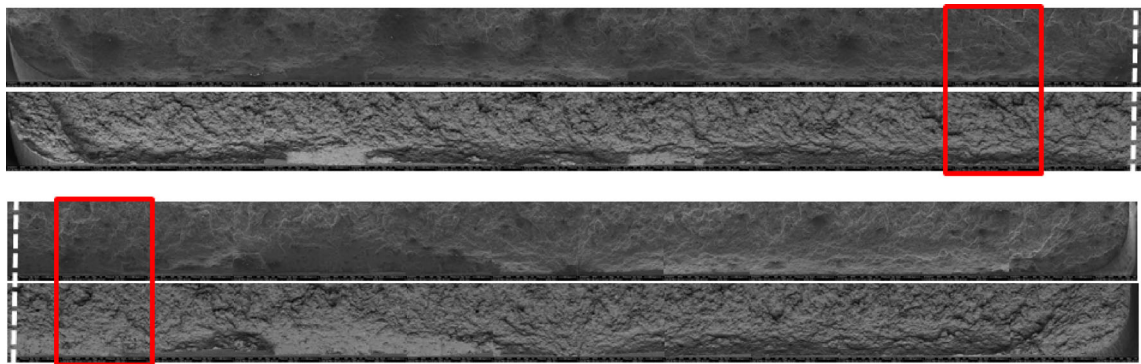
Fig. 13—SEM micrograph of the fracture surface of a sound casting (a_{RMS} = 71.46 m/s^2).
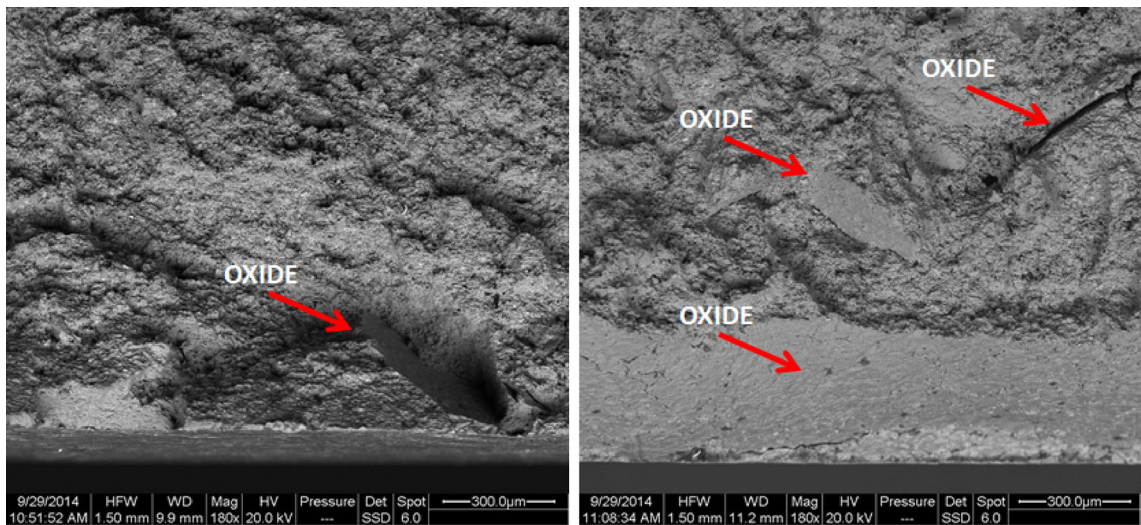

Fig. 14—180 times magnification of the marked zones of a scrap casting (a_{RMS} = 20.25 m/s^2).

particles, the energy associated to these forces is an influent parameter on destabilizing the preferential nucleation sites for defects.

In Figure 11, examples of a scrap and a sound casting (which will be deeply discussed in the following) are marked.

In Figures 12 and 13, SEM micrographs of the fracture surfaces of a scrap casting (the one in the first line of Table IV, with a_{RMS} = 20.25 m/s^2) and a sound casting (the one in the last line of Table IV, with a_{RMS} = 71.46 m/s^2), respectively, are shown. Both secondary electron and back-scattered electron images are
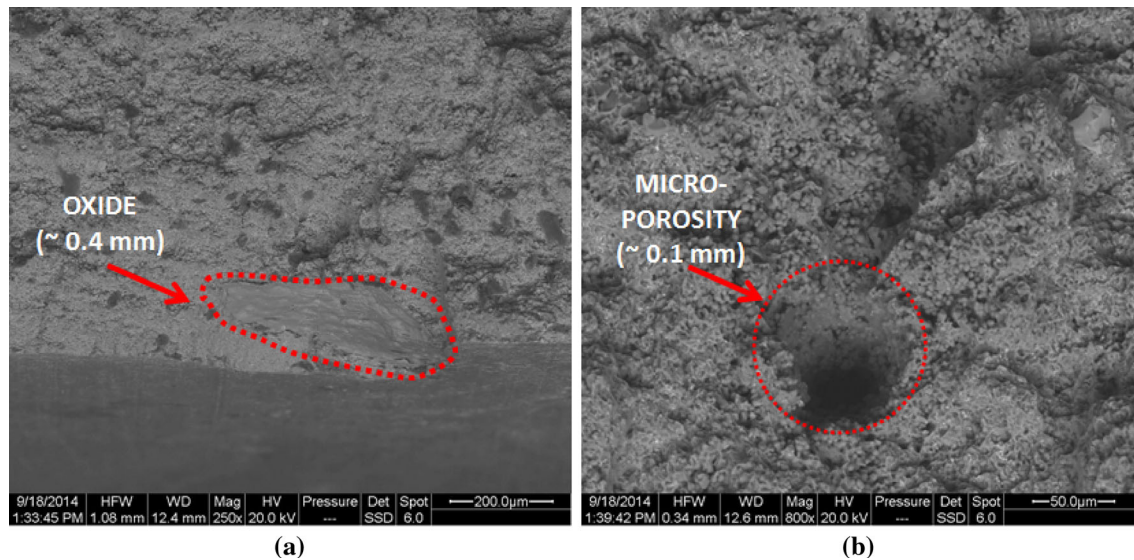
Fig. 15—Marked zones of a sound casting (a_{RMS} = 71.46 m/s^2) at (*a*) 250 times and (*b*) 800 times magnification.

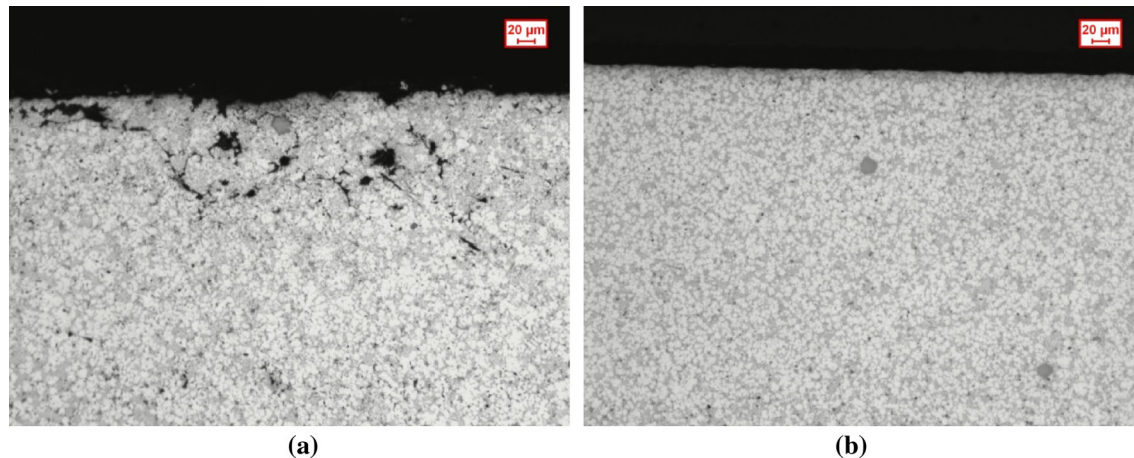

Fig. 16—Optical micrographs at 100 times magnification of the zone near the fracture surface of (*a*) a scrap casting (a_{RMS} = 20.25 m/s^2) and (*b*) a sound casting (a_{RMS} = 71.46 m/s^2).

represented for comparison. Magnifications of the marked zones of the abovementioned Figures 12 and 13 are then shown in Figures 14 and 15.

Figures from 12 through 15 highlight that the amount and the size of defects on the fracture surface are higher in the case of a scrap casting, justifying its lower bending peak load. Moreover, very large and detrimental oxides are usually located in sub-surface regions in the case of the scrap casting (see Figures 12 and 14), thus facilitating crack nucleation. In contrast, the fracture surface is more homogeneous and little defects are usually found in internal regions in the case of the sound casting with a consequent positive effect on the mechanical behavior (see Figures 13 and 15).

Finally, optical micrographs of Figure 16 confirm that the microstructure of a sound casting is more uniform than the one of a scrap casting. Moreover, Figure 16 (a) highlights that a lot of very dangerous defects, such as porosity and oxides, are concentrated

just below the surface of the scrap casting, thus compromising its mechanical behavior.

IV. CONCLUSIONS

This work has been focused on the identification and the definition of some parameters affecting the casting quality, by just analyzing the plunger motion. The meaningful parameters, which have been obtained through a systematic approach and by taking advantage of numerical processing of the plunger displacement time-history, are denoted as kinematic parameters and summarized as follows:

- the root mean square plunger acceleration in the second-stage a_{RMS}, which represents the average value of inertial forces related to the plunger motion;
- the integral of the cubic speed in the whole cycle E_f, which represents the energy associated to the flow

forces due to the contact between the melt and the wall of the die/chamber or some solid particles (such as oxides or inclusions), which are proportional to the square speed.

Given the integral nature of the HPDC process, the experimental analysis has confirmed that the two parameters having an integral mathematical nature (and hence accounting for the whole process or for some significant time intervals) are meaningful. As a matter of fact, they explain both the static mechanical properties and the percentage of porosity, as demonstrated by the application of statistical methods. Finally, the microscopic analysis reveals that by increasing a_{RMS} and E_f, the percentage of oxides decreases.

Further improvement of the model, to include upset pressure and temperature parameters, as well as development of analytical models for the a priori optimization of the HDPC process, will be proposed in future researches of the authors.

ACKNOWLEDGMENTS

REFERENCES

1. L. Wang, P. Turnley, and G. Savage: *J. Mater. Process. Technol.*, 2011, vol. 211, pp. 1510–15.
2. J.A. Francis and G.M.D. Cantin: *Mater. Sci. Eng. A*, 2005, vol. 407A, pp. 322–29.
3. F. Bonollo, E. Fiorese, G. Timelli, L. Arnberg, and A.R. Adamane: 71st World Foundry Congress: Advanced Sustainable Foundry, WFC 2014.
4. A.R. Adamane, L. Arnberg, E. Fiorese, G. Timelli, and F. Bonollo: *Int. J. Metalcasting*, 2015, vol. 9 (1), pp. 43–53.
5. C. Thibault and M. Funke: *Hydraul. Pneum.*, 2000, vol. 53 (10), pp. 51–54.
6. G.O. Verran, R.P.K. Mendes, and L.V.O. Dalla Valentina: *J. Mater. Process. Technol.*, 2008, vol. 200, pp. 120–25.
7. M.S. Dargusch, G. Dour, N. Schauer, C.M. Dinnis, and G. Savage: *J. Mater. Process. Technol.*, 2006, vol. 180, pp. 37–43.
8. D.R. Gunasegaram, B.R. Finnin, and F.B. Polivka: *Mater. Sci. Technol.*, 2007, vol. 23 (7), pp. 847–56.
9. R. Lumley, N. Deeva, and M. Gershenzon: *Int. J. Metalcasting*, 2011, vol. 5 (3), pp. 37–56.
10. Ł. Pałyga, M. Stachowicz, and K. Granat: *Arch. Foundry Eng.*, 2015, vol. 15 (2), pp. 85–90.
11. Z.P. Guo, S.M. Xiong, B.C. Liu, M. Li, and J. Allison: *Metall. Mater. Trans. A*, 2008, vol. 39A, pp. 2896–2905.
12. A. Hamasaiid, G. Dour, M.S. Dargusch, T. Loulou, C. Davidson, and G. Savage: *Metall. Mater. Trans. A*, 2008, vol. 39A, pp. 853–64.
13. L.W. Garber: *Die Cast. Eng.*, 1982, vol. 26 (3), pp. 14–15.
14. R. Zamora, F. Faura, J. López, and J. Hernández: *Int. J. Adv. Manuf. Technol.*, 2007, vol. 33 (3–4), pp. 266–76.
15. A.J. Nikroo, M. Akhlaghi, and M.A. Najafabadi: *Int. J. Adv. Manuf. Technol.*, 2009, vol. 41, pp. 31–41.
16. A. Krimpenis, P.G. Benardos, G.C. Vosniakos, and A. Koukouvitaki: *Int. J. Adv. Manuf. Technol.*, 2006, vol. 27 (5–6), pp. 509–17.
17. J. Zheng, Q. Wang, P. Zhao, and C. Wu: *Int. J. Adv. Manuf. Technol.*, 2009, vol. 44 (7–8), pp. 667–74.
18. R.V. Rao, V.D. Kalyankar, and G. Waghmare: *Appl. Math. Model.*, 2014, vol. 38, pp. 5592–5608.
19. J.K. Kittur, M.N. Choudhari, and M.B. Parappagoudar: *Int. J. Adv. Manuf. Technol.*, 2015, vol. 77, pp. 211–24.
20. J.K. Kittur, G.M. Patel, and M.B. Parappagoudar: *Int. J. Metalcasting*, 2016, vol. 10 (1), pp. 70–87.
21. I. Palomba, D. Richiedei, and A. Trevisani: in: *Proceedings of 26th International Conference on Noise and Vibration Engineering (ISMA)*, P. Sas, H. Denayer, and D. Moens, eds., 2014, Leuven, Belgium, pp. 2899–2914.
22. S. Wu, L. Xie, J. Zhao, and H. Nakae: *Scr. Mater.*, 2008, vol. 58, pp. 556–59.
23. G. Dour, M. Dargusch, C. Davidson, and A. Nef: *J. Mater. Process. Technol.*, 2005, vol. 169, pp. 223–33.
24. P. Homayonifar, R. Babaei, E. Attar, S. Shahinfar, and P. Davami: *Int. J. Adv. Manuf. Technol.*, 2008, vol. 39, pp. 219–28.
25. N. Roy, A.M. Samuel, and F.H. Samuel: *Metall. Mater. Trans. A*, 1996, vol. 27 (2), pp. 415–29.
26. H.E. Merritt: *Hydraulic Control Systems*, Wiley, New York, 1967.
27. G. Boschetti, R. Caracciolo, D. Richiedei, and A. Trevisani: *Mech. Syst. Signal Process.*, 2013, vol. 34 (1–2), pp. 116–30.
28. D.C. Montgomery: *Design and Analysis of Experiments*, 8th ed., Wiley, New York, 2012.
29. S. Otarawanna, H.I. Laukli, C.M. Gourlay, and A.K. Dahle: *Metall. Mater. Trans. A*, 2010, vol. 41A, pp. 1836–46.
30. D.C. Montgomery and G.C. Runger: *Applied Statistics and Probability for Engineers*, Wiley, New York, 2010.
31. J.J. Faraway: *Linear Models with R*, CRC Press, Boca Raton, 2014.
32. L. Wu: *Mixed Effects Models for Complex Data*, Chapman and Hall/CRC, Boca Raton, 2009.
33. VDG Specification: Examples of microstructures with different pore contents. BDG-Reference Sheet, 2010, pp. 1–24.